Air-sea gas exchange in a seagrass ecosystem — results from a $^3He/SF_6$ tracer release experiment

Ryo Dobashi[1], David T. Ho[1]

[1]Department of Oceanography, University of Hawai‘i at Mānoa, 1000 Pope Road, Honolulu, Hawaii 96822, USA

Correspondence to: Ryo Dobashi (rdobashi@hawaii.edu)

Abstract. Seagrass meadows are one of the most productive ecosystems in the world and could play a role in mitigating the increase of atmospheric CO_2 from human activities. Understanding their role in the global carbon cycle requires knowledge of air-sea CO_2 fluxes and hence knowledge of the gas transfer velocity. In this study, gas transfer velocity and its controlling processes were examined in a seagrass ecosystem in south Florida. Gas transfer velocity was determined using the ^3He and SF_6 dual tracer technique in Florida Bay near Bob Allen Keys (25.02663°N, 80.68137°W) between 1 and 8 April 2015. The observed gas transfer velocity normalized for CO_2 in freshwater at 20° C, $k(600)$, was 4.8 ± 1.8 cm h^{-1}. The resulting gas transfer velocities were lower than previous experiments in the coastal and open oceans at the same wind speeds. Therefore, using published wind speed/gas exchange parameterizations would overpredict gas transfer velocities and CO_2 fluxes in this area. The deviation in $k(600)$ from other coastal and offshore regions was only weakly correlated with tidal motion and air-sea temperature difference, implying that wind must therefore still be the dominant factor driving gas exchange. The lower gas transfer velocity was most likely due to wave attenuation by seagrass and limited wind fetch in this area. A new wind speed/gas exchange parameterization is proposed ($k(600) = 0.143u_{10}^2$), which might be applicable to other seagrass ecosystems and wind fetch limited environments.

1 Introduction

Seagrass meadows are one of the most productive ecosystems in the world and stock as much as 4.2–8.4 PgC in their soils (Fourqurean et al., 2012). Because the organic carbon produced via photosynthesis easily sinks to the bottom and some of the organic carbon stays in the ocean as a refractory matter, seagrass meadows are expected to be blue carbon sinks that can help mitigate the increase of anthropogenic CO_2. Seagrasses are estimated to bury 45−190 g C m^{-2} yr^{-1}, a significantly higher rate compared to terrestrial forests (0.7−13.1 g C m^{-2} yr^{-1}; Mcleod et al., 2011; Duarte et al., 2005). Recently, the role of seagrasses in the global carbon cycle has been revisited, as CO_2 emissions from $CaCO_3$ production were found to be large (Howard et al., 2017; Van dam et al., 2021). Howard et al. (2017) examined the stock of organic and inorganic carbon in the soil of seagrass meadows in Florida Bay and southeastern Brazil, and found that the soils in both regions have more inorganic carbon than organic carbon and are sources of CO_2 to the atmosphere. Schorn et al. (2021) also reported that the seagrasses in the Mediterranean Sea emit 106 µmol m^{-2} d^{-1} methane, mainly from their leaves.

Knowledge of the gas transfer velocity (k) is needed to understand the role of seagrass ecosystems in the global carbon cycle, since air-sea CO_2 flux is a function of k and the air-sea difference in the partial pressure of CO_2 (pCO_2). There are several methods to determine k in the field. The $^3He/SF_6$ dual tracer technique, which we employed in this study, is a mass balance technique that involves injecting these tracers into the ocean and determining k by measuring the change in the ratio of the two gases with time. The direct flux techniques, such as the eddy covariance method, measure the CO_2 flux in the air and CO_2 concentration both in the sea and air to derive k. k can also be estimated from the transfer velocity of heat by assuming that the gas and heat transfer velocities are related by their diffusivities; however, the estimated gas transfer velocity from heat, k_H, have been found to overestimate the actual k (e.g., Atmane et al., 2004).

Because k is difficult to measure, it is often parameterized using easily and widely measured parameters such as wind speed. In deep offshore regions, wind is known to predict the gas transfer velocity well since wind creates waves and currents, which control turbulence and bubbles at the sea surface (Wanninkhof et al., 2009). Ho et al. (2018a) examined k in the Kaneohe Bay in Hawai‘i and showed that k can be estimated well by wind speed where the depth is deeper than 10 m. On the other hand, in shallow regions, other parameters become important as well (e.g., Ho et al., 2016; 2018b). Ho et al. (2016) showed that k could be estimated well by wind speed and current speed in a shallow tidal estuary in south Florida, because the current enhances bottom-generated turbulence. Ho et al. (2018b) examined k in emergent wetland where the depth < 1 m, and showed that k can be parameterized from heat flux, rain rate and current velocity there. In the case of rain, rain rate is included in the parameterization because rainfall increases subsurface turbulence and k (Ho et al., 1997a, 2000).

In Florida Bay, k has been estimated from commonly used wind speed/gas exchange parameterizations. Zhang and Fischer (2014) determined the air-sea CO_2 flux to be 3.93 ± 0.91 mol m^{-2} yr^{-1} in Florida Bay; they used the wind speed/gas exchange parameterization determined from bomb-produced ^{14}C inventory in the ocean by Wanninkhof (1992). Van Dam et al. (2020) estimated k by using heat as a proxy (k_H) in Florida Bay and found that k_H is lower compared with k derived from published wind speed/gas exchange parameterizations when wind shear is relatively strong, even though k_H is known to overpredict k. This finding suggests that previous wind speed/gas exchange parameterizations are unsuitable for the seagrass-dominated area and a specific parameterization for these fetch-limited environments is needed. In the study presented here, we use a $^3He/SF_6$ tracer release experiment to determine k in a shallow seagrass-dominated environment to understand processes that control k and to derive a parameterization for this environment.

2 Methods

2.1 Study site

Florida Bay is located in the southernmost part of Florida, USA. It is situated between the Everglades marsh and the Florida Keys, and covers approximately 2,000 km^2. In this bay, the average depth is less than 3.5 m, and the vertical extent of seagrasses is between 0.08 and 0.2 m (Sogard et al., 1989). *Thalassia testudinum* and *Laurencia* are the dominate seagrass and macroalgae, respectively, in the benthic communities, with an average standing crop of 63.6 and 8.9 g dry weight m^{-2}, respectively (Zieman et al., 1989). Seagrass density varies across the bay, and its standing crop is 0−20 g dry weight m^{-2} in summer around our study area (bottom figure in Fig. 1) (Zieman et al., 1989). The seagrasses in Florida Bay show seasonality, and their standing crop becomes larger in spring and summer and smaller in fall and winter (Zieman et al., 1999). The phytoplankton community is dominated by cyanobacteria, diatoms, and dinoflagellates (Philips and Badylak, 1996). Cyanobacteria blooms occur frequently in the central north region of the bay due to nutrient input from the land (Philips et al., 1999; Lavrentyev et al., 1998). Wind persistently blows from southeast to northwest during summer and from north to south during winter (Wang et al., 1994). Current speed is about 0.02−0.14 m s^{-1} (Wang, 1998), and tidal amplitude is 0.1−0.4 m (Wang et al., 1994). The $^3He/SF_6$ tracer release experiments were conducted between 1 and 8 April 2015 near Bob Allen Keys (Fig. 1).

2.2 Tracer injection and underway SF_6 measurement

We injected ^3He and SF_6 at a ratio of 1:340 into the water at the study location (25.0107°N, 80.692°W; green star in Fig. 1) on 1 April 2015 for 1 minute via a length of diffuser tubing. After injection, we performed underway SF_6 measurements using an underway SF_6 analysis system (Ho et al., 2002) that measured SF_6 concentrations in the surface water every ~45 s. The system is composed of a gas extraction unit and an analytical unit. The gas extraction unit continuously removes SF_6 from the water for measurement using a membrane contactor. The other unit is composed of a gas chromatograph equipped with an electron capture detector (GC/ECD). Based on previous experiments, the system has a detection limit of 1×10^{-14} mol L^{-1} and an analytical precision of ±1% (Ho et al., 2018a). A personal computer displayed the SF_6 concentrations in real time. This provided a spatial distribution of the SF_6 patch, which guided the boat navigation. Around the center of the patch, we conducted discrete ^3He and SF_6 sampling (see below).

2.3 Discrete ^3He and SF_6 measurements:

We collected 16 ^3He samples (~40 mL each) at 26 stations in copper tubes mounted in aluminum channels and sealed at the ends with stainless steel clamps between April 1 and 8 2015 (yellow triangles in Fig. 1). In the shore-based laboratory at the end of the experiment, ^3He and other gases were extracted from the water in the copper tubes and transferred to flame-sealed glass ampoules. We measured ^3He concentration using a He isotope mass spectrometer (Ludin et al., 1998). 84 discrete SF_6 samples were taken at the same stations (yellow triangles in Fig. 1) using 50-mL glass syringes and submerged in water in a cooler until measurement back on shore at the end of each day. SF_6 was extracted by headspace technique and measured on a GC/ECD as described by Wanninkhof et al. (1987). We used the mean ^3He and SF_6 concentration for each day to determine k, so there are six $^3He/SF_6$ data points between April 3 and 8 (Fig. 2f).

2.4 Measurements of wind, temperature, salinity and tide

We measured wind speed, wind direction, and air temperature at ~5 m above sea level every 10 s using a sonic anemometer (Vaisala WMT700) near Bob Allen Keys (25.02663°N, 80.68137°W; blue dot in Fig. 1). The air temperature was averaged every 1 h to calculate the air-sea temperature difference (sea temperature minus air temperature). Hourly tidal amplitude, water surface temperature, and salinity data from the same site (blue dot in Fig. 1) between 2015 and 2019 were obtained from Everglades National Park (https://www.ndbc.noaa.gov/). The tidal amplitude was measured using a digital shaft encoder (WaterLog H331). Water temperature and salinity were measured using multiparameter sondes (Hydrolab Quanta until 5 March 2019; OTT-Hydromet OTT-PLS-C thereafter). Additional wind speeds measured using a sonic anemometer (Vaisala WXT532) at ~3 m above the sea level at 25.07209°N, 80.73511°W (pink square in Fig. 1, 7.4 km away from the blue dot) between 2015 and 2019 were obtained from Everglades National Park to compare *k* derived from this study and *k* estimated from published parameterizations.

Wind speed data were extrapolated to 10 m above the sea level using the equation below (Amorocho and DeVries, 1980):

$$u_z = u_{10}\left(1 - C_{10}^{\frac{1}{2}}\kappa_c^{-1}\ln(10/z)\right) \tag{1}$$

where u_z is the wind speed at height z, κ_c is the von Kármán constant (0.41), C_{10} is the surface drag coefficient of wind at 10 m height (1.3×10^{-3}) (Stauffer, 1980).

2.5. Underway pCO_2 Measurements

We measured the pCO_2 along the boat track (red dots in Fig. 1) using an underway system based on the design of Ho et al. (1997b) and incorporating the suggestions from Pierrot et al. (2009). Water was pumped through a thermosalinograph (TSG) into a showerhead equilibrator, and a high precision thermistor measured the temperature. The gas was dried by Nafion and $Mg(ClO_4)_2$ dryers, and was continuously circulated through a non-dispersive infrared (NDIR; LI-COR LI-840A) analyzer. We stopped the flow during measurement and vented the NDIR cell to the atmosphere. The interval between measurements was 41 s. Atmospheric air was taken from an inlet at the bow of the boat through a length of aluminum/plastic composite tubing (Dekabon), and was diverted into the NDIR analyzer at specific times (every ~72 min). We calibrated the analyzer at regular time intervals (~72 min) with a 511 ppm CO_2 standard calibrated with a primary standard from NOAA/ESRL/GMD and a CO_2-free reference gas (UHP N_2 passed through soda lime to remove CO_2). In total, 1,261 and 13 xCO_2 data were taken from the water and air, respectively. With measured mole fraction of CO_2 (xCO_2), barometric pressure (P), and water vapor pressure at water surface temperature (Vp), we calculated the water and atmospheric pCO_2 by applying the following expression (DOE, 1994): $pCO_2 = (P - Vp) \times xCO_2$. pCO_2 values were corrected for temperature shifts in the sample from the intake point (i.e., as measured by the TSG) to the pCO_2 system using an empirical equation proposed by Takahashi et al. (1993). Fugacity of CO_2 (fCO_2) was calculated by $fCO_2 = \alpha \times pCO_2$, where α is an activity coefficient calculated from a formula in Wanninkhof and Thoning (1993). Additional fCO_2 data were obtained from National Oceanic and Atmospheric Administration (NOAA) (https://www.pmel.noaa.gov/) at 24.90°N, 80.62°W (cyan diamond in Fig. 1, 15 km away from the blue dot). CO_2 flux between air and water was calculated with solubility (K_0) and fCO_2 using the equation below:

$$F = kK_0(fCO_{2water} - fCO_{2air}), \quad (2)$$

where the K_0 was calculated from the measured temperature and salinity (Weiss, 1974).

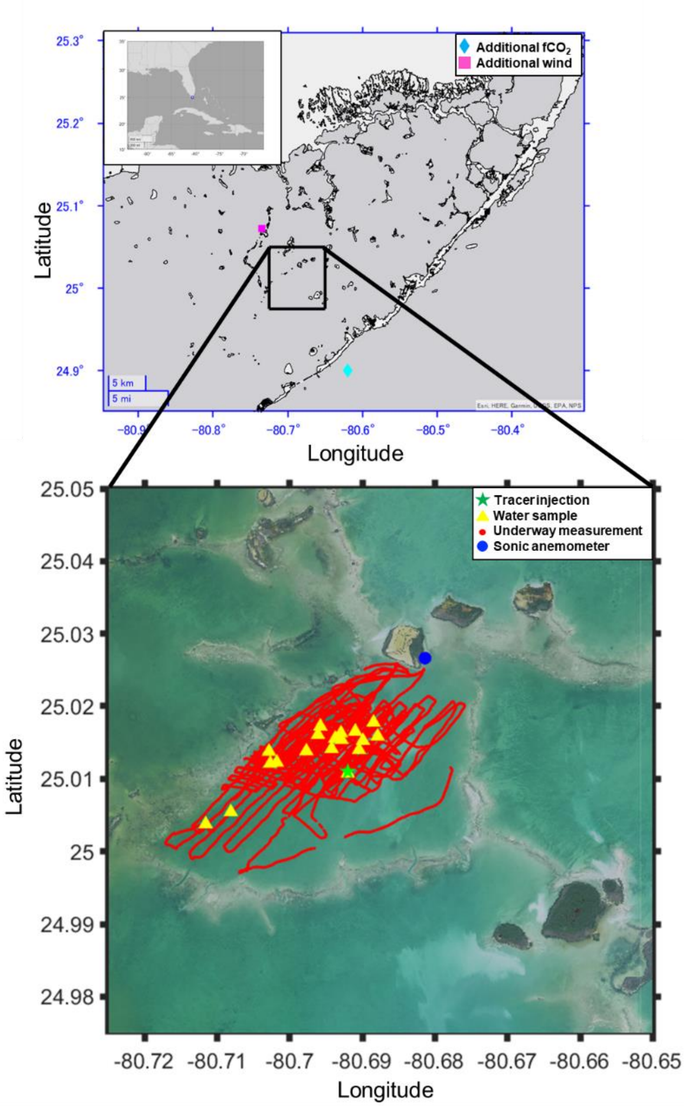

Fig. 1 Map of the study area. Green star is the ^3He and SF_6 injection location; red dots are the boat track where underway measurement was conducted for pCO_2 and SF_6; blue dot is the location where wind velocity, air temperature, water temperature, salinity and tidal amplitude were measured; yellow triangle are the stations where discrete samples for ^3He and SF_6 were taken; pink square is where additional wind velocity was measured; and aqua diamond indicates where additional fCO_2 were measured. Note that water temperature, salinity, tidal amplitude and additional wind velocity were obtained from Everglades National Park, and additional fCO_2 were obtained from NOAA. Map data are generated by MATLAB geobasemap “darkwater” and downloaded from Fish and Wildlife Research Institute (https://myfwc.com/research/) and NOAA (https://www.noaa.gov/)

2.6. Gas transfer velocity measurement

The two tracers, ^3He and SF_6, were injected together into the mixed layer at a constant ratio, and the ratio of $^3He/SF_6$ was measured over time as described above. The technique relies on the well-tested assumption that patch dilution, such as by horizontal mixing, affects the individual tracer concentrations but does not alter the $^3He/SF_6$ ratio; the only process that changes the $^3He/SF_6$ ratio is air-sea gas exchange. The gas transfer velocity for ^3He, $k_{^3\mathrm{He}}$, can be determined as follows (Wanninkhof et al., 1993):

$$k_{^3\mathrm{He}} = -\left(1 - \left(\mathrm{Sc}_{\mathrm{SF_6}}/\mathrm{Sc}_{^3\mathrm{He}}\right)^{-1/2}\right)^{-1} h \frac{\mathrm{d}}{\mathrm{dt}}\left(\ln\left({}^3\mathrm{He_{exc}}/\mathrm{SF_6}\right)\right) \quad (3)$$

where $\mathrm{Sc}_{\mathrm{SF_6}}$ and $\mathrm{Sc}_{^3\mathrm{He}}$ are the Schmidt numbers (i.e., the kinematic viscosity of water divided by diffusion coefficient of the gas in water) for SF_6 and ^3He, respectively (see section 2.7). *h* is the measured water depth in Florida Bay, adjusted for tidal variation. $^3He_{exc}$ is the ^3He in excess of solubility equilibrium with the atmosphere (used interchangeably with ^3He here). The gas transfer velocity measured during this experiment is normalized to *k*(600), where 600 corresponds to *Sc* number of CO_2 in freshwater at 20°C:

$$k(600) = k_{^3\mathrm{He}}\left(600/\mathrm{Sc}_{^3\mathrm{He}}\right)^{-1/2}. \quad (4)$$

2.7 Calculation of *Sc* number

In the literature, *Sc* is often calculated from a compilation by Wanninkhof (2014). However, because the salinity in Florida Bay is 40, which is higher than the range provided by Wanninkhof (2014), we have re-calculated *Sc* for an extended range here. In our calculation, the kinematic viscosity for fresh water and seawater are derived using equations given by Sharqawy et al. (2010). Molecular diffusion coefficients of various gasses for freshwater were calculated using empirical equations derived from previous studies (Jähne et al., 1987; Wilke and Chang, 1955; Hayduk and Laudie, 1974; King and Saltzman, 1995; Saltzman et al., 1993; Zheng et al., 1998; De Bruyn and Saltzman, 1997). While the effect of temperature on molecular diffusion coefficient is well investigated, the effect of salinity has been the subject of fewer studies. SF_6, methyl bromide (CH_3Br), and trichlorofluoromethane (CFC-11) do not have significant differences in diffusion coefficients between fresh water and a 35 g L^{-1} sodium chloride (NaCl) solution (King and Saltzman, 1995; De Bruyn and Saltzman, 1997; Zheng et al., 1998). However, diffusion coefficients for methane (CH_4), dichlorodifluoromethane (CFC-12), and He in seawater are 4−7% less than the coefficients in freshwater (Jähne et al., 1987; Saltzman et al., 1993; Zheng et al., 1998). To represent the dependence of molecular diffusion coefficients on salinity for gasses except for SF_6, CH_3Br and CFC-11, we linearly inter/extrapolated the molecular diffusion coefficients for various salinities by assuming that the diffusion coefficients decrease by 6% when the salinity is 35, compared with freshwater (Jähne et al., 1987; Wanninkhof, 2014). Molecular diffusion coefficients for a salinity of 40 are about 7% smaller compared to the coefficients for freshwater based on this assumption.

Least-squares fourth-order polynomial fit, including the effect of salinity, was produced to predict the *Sc* numbers at various temperatures and salinities (Table 1).

Table 1. Coefficients for a least-squares fourth-order polynomial fit of Schmidt number versus salinity and temperature for various salinity and temperatures from 0 to 40°C.

Gas	**A**	**a**	**B**	**b**	**C**	**c**	**D**	**d**	**E**	**e**	**Sc number (20°C, 0 PSU)**	**Sc number (20°C, 35 PSU)**
^3He	334.38	0.90630	-17.566	-0.040902	0.53156	0.0011076	-0.0094081	-1.8342×10^{-5}	7.1715×10^{-5}	1.3483×10^{-7}	132	146
He	377.10	1.1097	-19.810	-0.050665	0.59949	0.0013852	-0.010610	-2.3081×10^{-5}	8.0880×10^{-5}	1.7028×10^{-7}	149	166
Ne	764.44	2.2495	-43.818	-0.11364	1.3943	0.0032933	-0.025331	-5.652×10^{-5}	0.00019561	4.2289×10^{-7}	274	306
Ar	1876	5.5663	-131.69	-0.32458	4.9298	0.010744	-0.099518	-0.00020223	0.00081784	1.5998×10^{-6}	549	619
O_2	1733.6	5.1437	-121.69	-0.29994	4.5556	0.0099283	-0.091963	-0.00018688	0.00075576	1.4784×10^{-6}	507	572
N_2	2080.6	6.1735	-146.06	-0.35999	5.4677	0.011916	-0.11037	-0.00022429	0.00090706	1.7743×10^{-6}	609	687
Kr	2036.2	5.9923	-133.13	-0.35181	4.5886	0.011183	-0.087051	-0.00020169	0.00068746	1.5474×10^{-6}	623	695

Xe	2688.8	7.9128	-181.43	-0.48144	6.3779	0.015655	-0.12233	-0.00028594	0.0009717	2.2082×10^{-6}	788	880
CH_4	1900.3	5.5923	-119.02	-0.31267	3.9947	0.009639	-0.074686	-0.00017095	0.00058531	1.3002×10^{-6}	614	685
CO_2	1914.2	5.6330	-123.18	-0.32481	4.2040	0.010208	-0.079322	-0.00018296	0.00062463	1.3992×10^{-6}	598	667
N_2O	2127	6.3112	-149.31	-0.36802	5.5897	0.012182	-0.11284	-0.00022929	0.0009273	1.8139×10^{-6}	622	702
Rn	3154.1	9.2820	-220.51	-0.58779	7.9274	0.019612	-0.15397	-0.00036344	0.0012313	2.8283×10^{-6}	880	982
SF_6	3024	3.0926	-193.63	-0.14258	6.5878	0.0035655	-0.12409	-5.3058e$\times10^{-5}$	0.00097626	3.5673×10^{-7}	950	996
DMS	2582.0	7.5983	-160.71	-0.42182	5.3733	0.012946	-0.10025	-0.00022905	0.00078480	1.7401×10^{-6}	841	938
CFC-12	3460.3	10.183	-225.72	-0.5963	7.7688	0.018924	-0.14727	-0.00034099	0.0011625	2.6148×10^{-6}	1061	1184
CFC-11	3446.9	3.5251	-214.51	-0.15589	7.1717	0.0037741	-0.1338	-5.4896×10^{-5}	0.0010474	3.6378×10^{-7}	1123	1176
CH_3Br	2101	2.1487	-133.27	-0.097717	4.5081	0.0024177	-0.084644	-3.571×10^{-5}	0.00066483	2.3896×10^{-7}	668	700
CCl_4	3973.3	11.789	-278.92	-0.68747	10.442	0.022756	-0.21078	-0.00042832	0.0017322	3.3884×10^{-6}	1163	1312

Sc = A+aS + (B+bS)T + (C+cS)T^2 + (D+dS)T^3 + (E+eS)T^4 (T in °C). The last two columns are the calculated Schmidt number for 20°C, and salinities of 0 and 35 as examples, respectively. The diffusion coefficients, denominators of *Sc*, are derived from the following: ^3He, He, Ne, Kr, Xe, CH_4, CO_2 and Rn measured by Jähne et al. (1987); Ar, O_2, N_2, N_2O, and CCl_4 fit from Wilke and Chang (1955) adapted by Hayduk and Laudie (1974); SF_6 measured by King and Saltzman (1995); DMS measured by Saltzman et al. (1993); CFC-11 and CFC-12 measured by Zheng et al. (1998); CH_3Br measured by De Bruyn and Saltzman (1997). *Sc* numbers for temperature of 20°C and salinity of 35 become larger than *Sc* numbers for temperature of 20°C and salinity of 0 by 4.7–4.8% for SF_6, CFC-11 and CH_3Br and 10.8–12.8% for other gasses, respectively. Note that the fits are based on simple assumptions (see section 2.7), and the dependence of *Sc* on salinity needs to be investigated further in the future.

2.8 Modeling the decrease of $^3He/SF_6$ ratio

The decrease of the tracer ratio was compared to the decrease predicted by published wind speed/gas exchange parameterizations to assess the validity of these parameterization for the study area. Under the assumption that air-sea gas exchange is the only process that alters the $^3He/SF_6$ ratio in the water, the change in $^3He/SF_6$ ratio during this experiment can be modeled by an analytical solution to equation (3):

$$\left({}^3\mathrm{He}/\mathrm{SF_6}\right)_t = \left({}^3\mathrm{He}/\mathrm{SF_6}\right)_{t-1} \exp\left(-\frac{k_{\,{}^3\mathrm{He}}\Delta t}{h}\left(1-\left(\mathrm{Sc_{SF_6}}/\mathrm{Sc}_{\,{}^3\mathrm{He}}\right)^{-1/2}\right)\right) \tag{5}$$

where $(^3He/SF_6)_t$ is the ^3He to SF_6 ratio at time t and $(^3He/SF_6)_{t-1}$ is the ratio at the previous time step. $k_{\,^3\mathrm{He}}$ is predicted from wind speeds measured during this experiment and existing parameterizations. The skill of the parameterizations to predict the measured $^3He/SF_6$ during this experiment is evaluated in terms of the coefficient of variation of the root mean square error (cvRMSE):

$$\mathrm{cvRMSE} = \frac{\sqrt{\frac{1}{\mathrm{N}}\sum_{\mathrm{n}=1}^{\mathrm{N}}\left(\mathrm{R_{mod}^n}-\mathrm{R_{obs}^n}\right)^2}}{\overline{\mathrm{R_{obs}}}}, \tag{6}$$

where R_{obs}^n and R_{mod}^n are the observed and modeled $^3He/SF_6$ tracer ratios, respectively, and N is the number of stations sampled after the initial sampling (5 for table 2 and 2 for Fig. 5e). The ability of commonly used parameterizations, including the quadratic relationships of Wanninkhof (1992), Nightingale et al. (2000), and Ho et al. (2006), the exponential relationship of Raymond and Cole (2001), and the hybrid parameterization of Wanninkhof et al. (2009) to predict *k* in Florida Bay was evaluated by examining the cvRMSE. Equation (6) was also used to derive the optimal coefficients (A) for a quadratic ($k = Au_{10m}^2$) parameterization by minimizing the cvRMSE. We regarded A with minimum cvRMSE as the best coefficient for parameterization.

3. Results and discussion

3.1 Environmental parameters

During the experiment, wind direction was predominately from the east, and wind speeds increased towards the latter part of the study period (Fig. 2a). The mean and the standard deviation of the wind speed during the study period was 5.5 ± 2.0 m s^{-1} (range=0.12–12 m s^{-1}). Mean water temperature showed diurnal pattern with a mean and standard deviation of 26.3 ± 1.3°C (Fig. 2b). The diurnal pattern of the air temperature was weak, as the mean and standard deviation were 25.1 ± 0.6°C. The air-sea temperature difference showed diurnal cycles, which was mainly driven by the diurnal cycle of the sea temperature, consistent with observations by Van Dam et al. (2020). Salinity was consistent throughout the study period (41 ± 0.1) (not shown). The tide consistently showed semidiurnal cycles with an amplitude of ≤ 0.2 m throughout the study period.

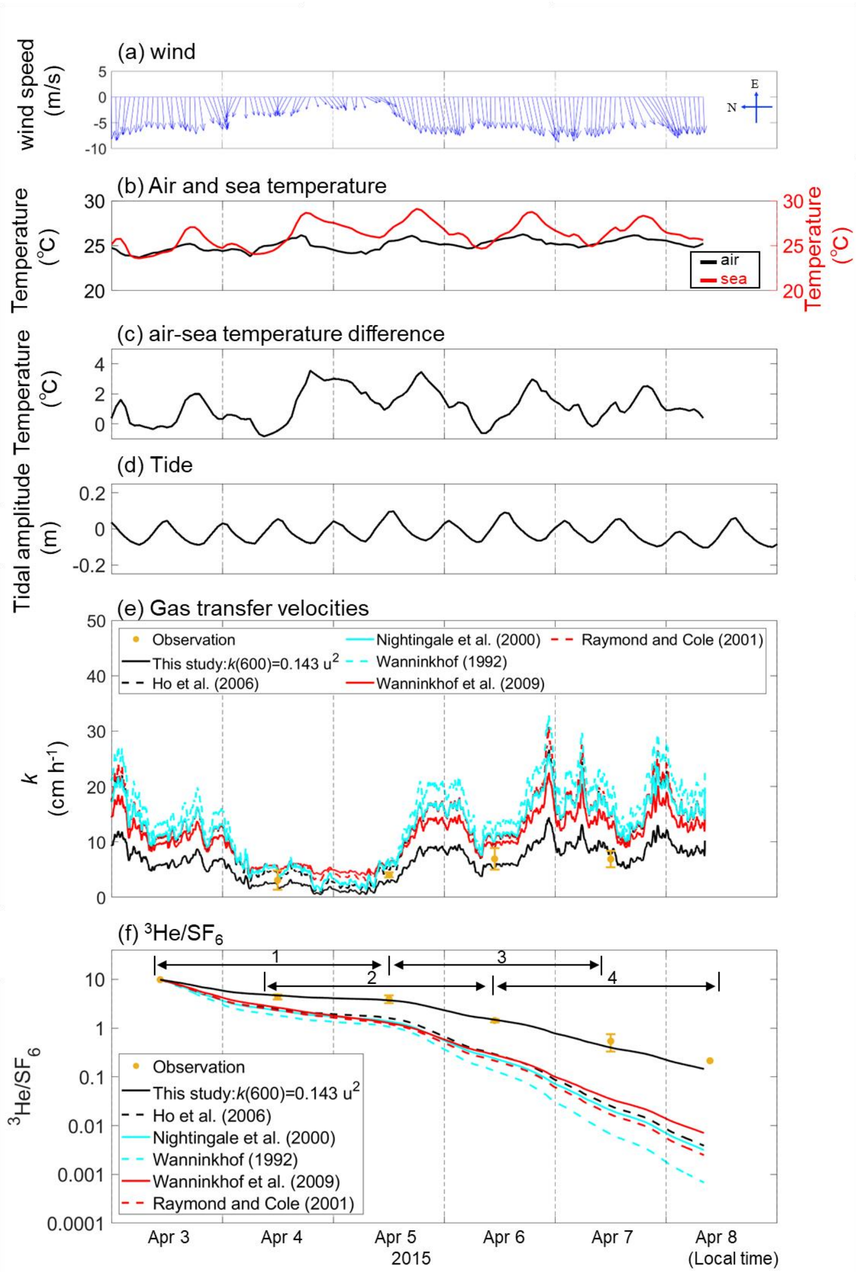

Fig. 2 Time series of (a) hourly averaged wind vector at 10 m height (m s^{-1}), (b) water temperature and air temperature (°C), (c) temperature difference (water temperature minus air temperature; units: °C), (d) tidal amplitude (units: m) and (e) measured and estimated gas transfer velocities for CO_2 at in-situ temperature and salinity and (f) measured and modeled change in $^3He/SF_6$. Note that the wind direction is towards the north when the vector is towards the left. The time zone is local time. The numbers in (f) indicate the periods corresponding to the x-axis in Fig. 5.

3.2 Gas transfer velocity in Florida Bay

The measured $k(600)$ was 4.8 ± 1.8 cm h^{-1} (mean ± s.d.) (Fig. 3), which was lower than previous studies conducted in coastal and open oceans at the same wind speed (Fig. 3 of Ho & Wanninkhof, 2016). A new parameterization was produced based on results from this experiment by minimizing the cvRMSE of $A \cdot u_{10}^2$, where A is a coefficient (Fig. 4):

$$k(600) = 0.143u_{10}^2 \quad (7)$$

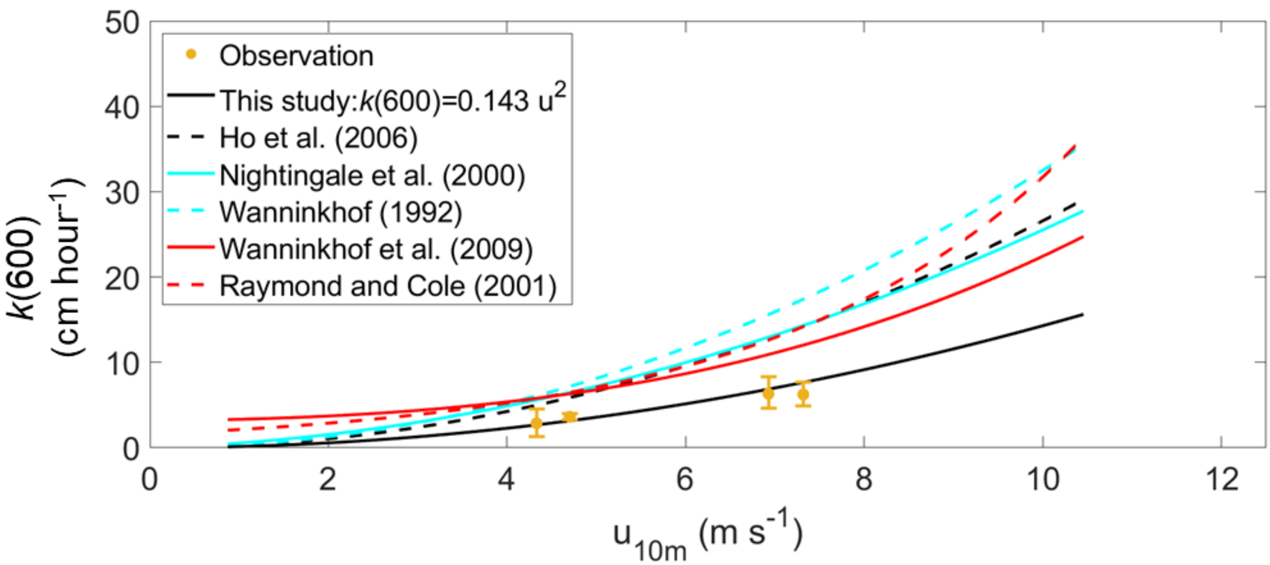

Fig. 3 Measured and modeled $k(600)$ (units: cm h^{-1}) with wind speed at 10 m height (units: m s^{-1}).

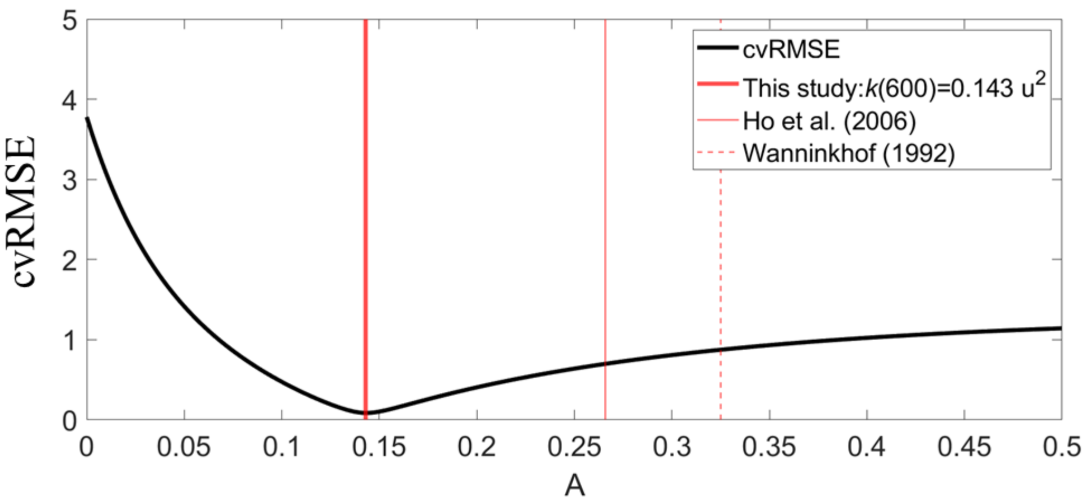

Fig. 4 The relationship between cvRMSE and the coefficient A in the equation $k(600)=A\ u_{10}^2$. Three vertical lines indicate the coefficients derived from this study, as well as those of Ho et al. (2006) and Wanninkhof (1992) from left to right. Note that $k(660)$ in Wanninkhof (1992) was converted to $k(600)$ by assuming that they scale as Sc to the power of −1/2.

The cvRMSE between the measured $^3He/SF_6$ and this new parameterization, equation (7), was 8.6%, while the cvRMSEs calculated from previously published wind speed/gas exchange parameterizations were more than 70% (Table 2). The coefficient of 0.143 was 46% and 56% lower than the $k(600)$ of 0.266 and 0.325 from Ho et al. (2006) and Wanninkhof (1992), respectively (Fig. 3). The result of previous studies which used the parameterization of Wanninkhof (1992) in Florida Bay was modified in section 3.2. The estimated k for CO_2 at in-situ temperature and salinity derived from equation (7) was 6.3±3.3 cm h^{-1}, while all the published parameterizations estimated over 10 cm h^{-1} on average between 3 and 8 April 2015(Fig. 2e). k for CO_2 at in-situ temperature and salinity between 2015 and 2019 were also calculated using the equation (7) and the previously published parameterizations (Table 3). Annual averaged k ranged between 3.7–4.3 cm h^{-1} in Florida Bay between 2015 and 2019, while published parameterization would yields values of 6.9–11.6 cm h^{-1}.

The deviations of observed $^3He/SF_6$ and modeled $^3He/SF_6$ derived from published parameterizations become larger with time, as shown in Figure 2f. This means that the published parameterizations overpredict k in Florida Bay, which is consistent with the result of Van Dam et al. (2020).

Table 2. Gas transfer velocities determined from published parameterization.

References	**Parameterization**	**Mean $k(600)$ (cm h^{-1})**	**cvRMSE**
This study	$k(600)= 0.143u_{10}^2$	5.5±3.0	8.6%
Ho et al. (2006)	$k(600)=0.266u_{10}^2$	10.2±5.5	70.0%
Nightingale et al. (2000)	$k(600)=0.333u_{10} + 0.222u_{10}^2$	10.4±5.2	76.0%

Wanninkhof (1992)	$k(660)=0.31u_{10}^2$	12.4±6.8	87.5%
Wanninkhof et al. (2009)	$k(660)=3+0.1u_{10} + 0.064u_{10}^2 + 0.011u_{10}^3$	9.4±3.8	73.1%
Raymond and Cole (2001)	$k(600)=1.58e^{0.3u_{10}}$	10.7±5.3	78.2%

The observed $k(600)$ was 4.8 ± 1.8 cm h^{-1} (average ± standard deviation). Note that $k(660)$ is converted to $k(600)$ by assuming that the scale by *Sc* to the power of –1/2.

Table 3. Gas transfer velocities of CO_2 at in-situ temperature and salinity in Florida Bay between 2015 and 2019 determined using the wind speed/gas exchange parameterization determined here and predicted using published parameterizations.

Parameters		2015	2016	2017	2018	2019	Between 2015 and 2019
Wind speed (m s^{-1})		4.2±2.4	4.4±2.6	4.1±2.7	4.4±2.5	4.7±2.4	4.4±2.5 (range=0–27.5)
Sea temperature (°C)		27.6±3.8	26.7±4.1	26.8±3.9	26.7±4.2	27.3±3.8	27.0±4.0 (range=13.2–36.2)
Salinity		40.5±4.0	34.1±3.6	34.7±5.2	33.0±2.7	39.5±2.9	36.3±4.8 (range=24.5–51.8)
Tidal amplitude (m)		0.16±0.03	0.17±0.03	0.18±0.06	0.18±0.03	0.18±0.03	0.17±0.04 (range=0.04–0.33)
Mean *k* for CO_2 (cm h^{-1})	This study	3.7±4.0	4.0±4.1	3.8±5.6	4.0±4.1	4.3±4.4	3.6±4.2 (range=0–108)
	Ho et al. (2006)	6.9±7.4	7.4±7.7	7.1±10.4	7.4±7.7	8.1±8.1	6.8±7.9 (range=0–202)
	Nightingale et al. (2000)	7.3±7.0	7.8±7.3	7.4±9.6	7.8±7.3	8.5±7.6	7.1±7.4 (range=0–176)
	Wanninkhof (1992)	8.4±9.1	9.0±9.4	8.7±12.8	9.1±9.4	9.9±9.9	8.3±9.6 (range=0–247)
	Wanninkhof et al. (2009)	7.8±5.4	8.1±5.5	8.2±10.1	8.1±5.7	8.6±6.0	7.4±6.4 (range=3.1–298)
	Raymond and Cole (2001)	8.5±8.9	8.9±9.1	11.6±86.2	9.1±10.4	9.7±10.0	8.7±36 (range=1.6–6127)

The standard deviation of Raymond and Cole (2001) were large in 2017 since wind speed was as high as 27.5 m s^{-1}, and *k* was as high as 6.1×10^3 cm h^{-1}.

Van Dam et al. (2020) estimated the air-sea gas transfer velocity using heat as a proxy (k_H) in Florida Bay. They found that k_H was lower than *k* calculated from published parameterization even though k_H is known to overpredict *k*. They suggested that the stratification due to temperature restricts air-sea gas exchange since the deviation between k_H and *k* from commonly-used parameterization was large when the air-sea temperature difference was large. To investigate the relationship between environmental parameters and the deviation between measured and estimated air-sea gas exchange, we examined the relationship between temperature difference and the deviation between observation and the models by calculating cvRMSE separately in four periods (Fig. 5). We found no clear relationship between the deviation and air-sea temperature difference. The deviation observed in Van Dam et al. (2020) might be due to the fact that k_H contains the air-sea temperature difference in its equation (equation 7 in Van Dam et al. 2020); k_H becomes smaller when the air-sea temperature difference is large and vice versa.

The new wind speed/gas exchange parameterization predicts the observed change in $^3He/SF_6$ well (Fig. 2f and Table 2), suggesting that wind is the dominant factor controlling gas exchange in this area. In Florida bay, waves are damped by seagrasses (Prager and Halley, 1999), which might be one of the causes of lower *k* in this study. There is also the possibility that limited wind fetch in this region led to relatively weak waves and turbulence compared to other regions, contributing to lower *k*. Wind fetch is limited in this region, since the wind mostly blows from east to west, and the Florida Keys restricts the water exchange between the bay and the Atlantic Ocean (Fig. 1 and Fig. 2a). There was almost no rainfall to affect *k* during the study period. Tidal amplitude was small (~0.1 m) (Fig. 2d), suggesting that the bottom-generated turbulence was weak.

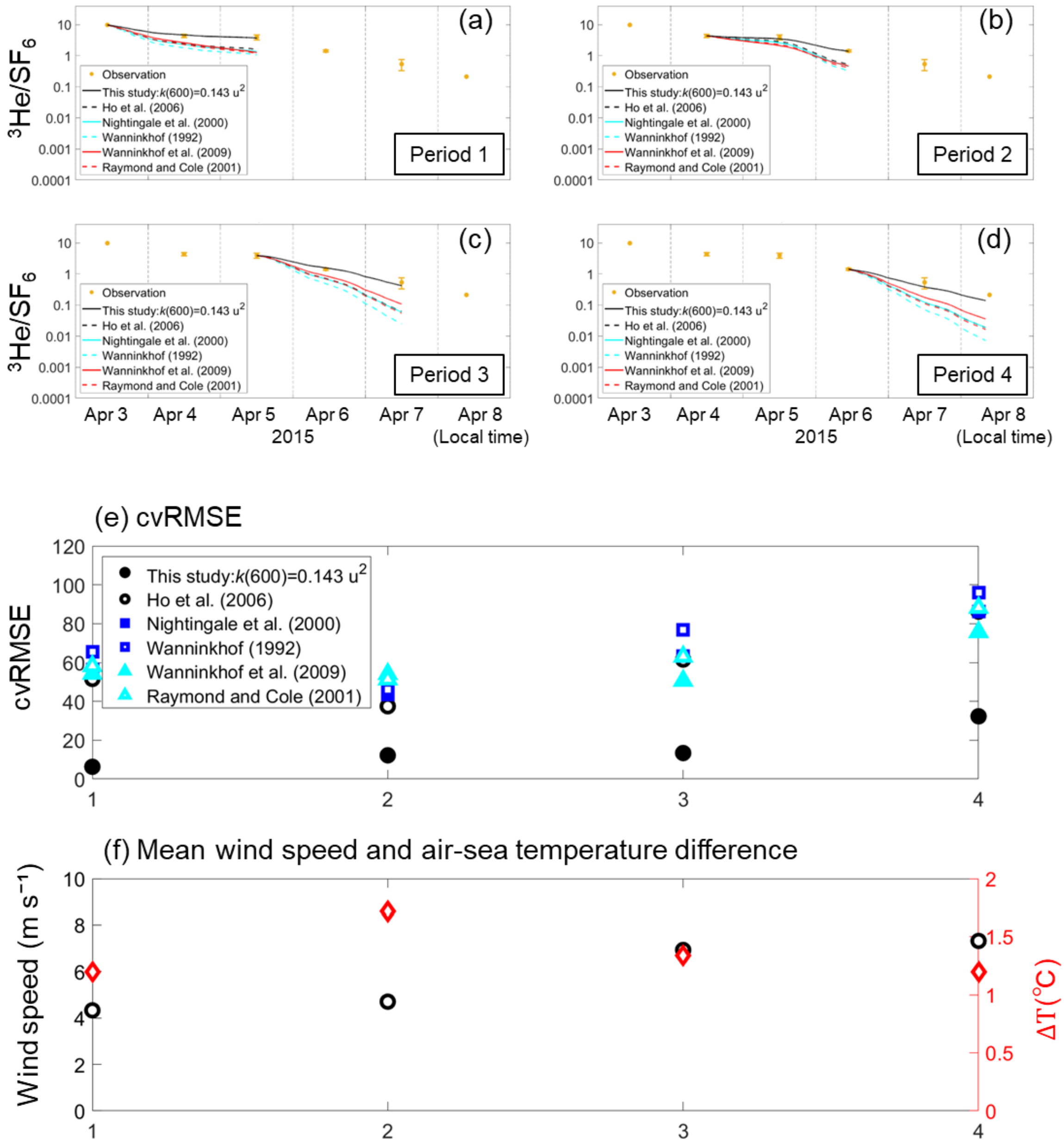

Fig. 5 Time series of measured and modeled change in $^3He/SF_6$ in (a) period 1, (b) period 2, (c) period 3, and (d) period 4 in Fig. 2f. $^3He/SF_6$ value is set to the starting point of each period. (e) The cvRMSE, (f) mean wind speed (m s^{-1}) and air-sea temperature difference (°C) during the period of 1–4. The x-axis represents the periods in Fig. 2f.

3.2 Implications for biogeochemistry

Although the experiment was conducted over a short period of 8 days, our new parameterization, equation (7), fit the observations well; This implies that equation (7) can be applied even in different seasons and years if the wind speed is in the range of 0.12–12 m s^{-1} and seagrass conditions are similar. The parameterization determined in this study should be applicable to other seagrass ecosystems as well, since seagrass ecosystems are typically in coastal regions. In these environments, waves are damped by seagrasses and limited fetch. This wind speed/gas exchange parameterization proposed here might be applicable not only in seagrass ecosystems but also in other wind-fetch limited areas. To assess the applicability of this new parameterization in other inland ecosystems, additional $^3He/SF_6$ dual tracer experiments will need to be conducted. Specifically, measuring the seagrass density and conducting dual-tracer experiment simultaneously is needed to relate the *k* and vegetation distribution.

The observed daytime pCO_{2water} and pCO_{2air} were 228 ± 16 and 393 ± 3 µatm, respectively (Fig. 6a). The pCO_{2water} of 228 ± 16 µatm was in the range shown by Zhang and Fischer (2014), who examined the pCO_{2water} in whole basin of the Florida Bay from 2006 to 2012, and showed that pCO_{2water} minima was ~200 µatm in April (Fig. 3 of Zhang and Fischer 2014). Since the observed pCO_{2water} was lower than pCO_{2air}, CO_2 goes from air to the sea during the daytime in the observation period (between 3 and 8 April 2015). The calculated CO_2 flux using the measured pCO_2 difference and modeled *k* in this study (Black solid line in Fig. 2e) was –4.4 ± 2.6 mmol m^{-2} day^{-1} (negative value means CO_2 goes from the air to the sea) (Fig. 6b). Although we did not conduct pCO_2 measurement during the night and so the calculated value is biased toward daytime, the daily averaged pCO_{2water} and CO_2 flux during the whole observation period would still be lower than pCO_{2air} and negative, respectively, considering that the observed pCO_2 was as low as 228 µatm and the CO_2 flux at the NOAA station (aqua diamond in Fig. 1) was always negative with diurnal fCO_{2water} amplitude of 25–53 µatm between April 3 and 8, 2015.

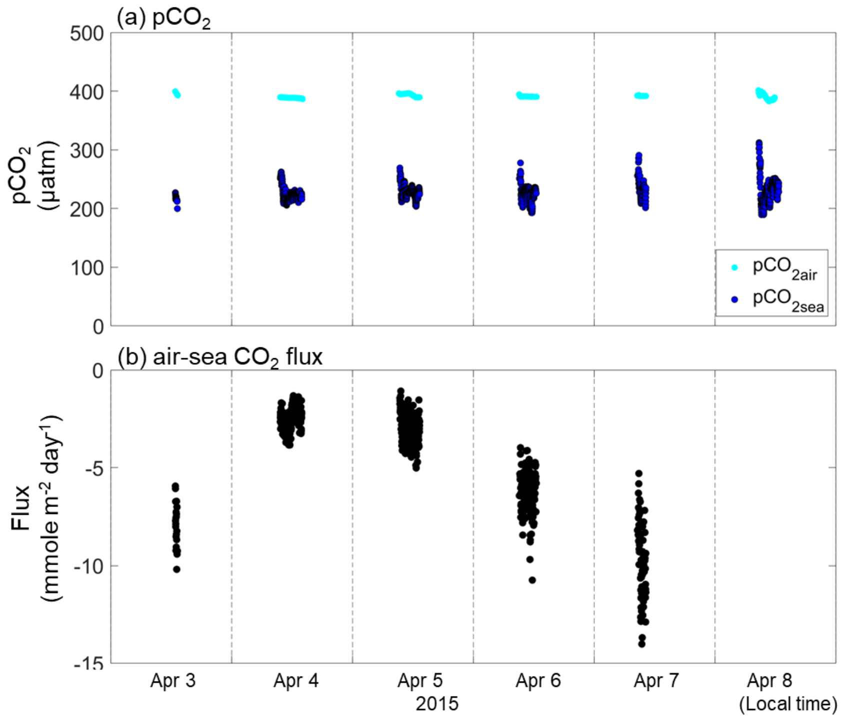

Fig. 6 Time series of (a) measured pCO_{2water} (blue dots) and pCO_{2air} (cyan dots) (units: µatm), (b) calculated CO_2 flux (units: mmole m^{-2} day^{-1}). The time zone is local time.

Annual averaged CO_2 flux is, however, known to be from the water to the air in Florida Bay (e.g., Zhang and Fischer, 2014; Van dam et al., 2021). The pCO_2 and CO_2 flux in Florida Bay are suggested to have seasonality due to cyanobacteria blooms (Zhang and Fischer, 2014). The seasonality of seagrasses may also contribute to the seasonality of pCO_2 and CO_2 flux, as its productivity also shows seasonality (higher in spring and summer and lower in fall and winter) (Zieman et al., 1999). Zhang and Fischer (2014) measured the pCO_{2water} for the whole area of the Florida Bay and estimated the CO_2 flux in Florida Bay to be 3.93 ± 0.91 mol m^{-2} yr^{-1} using the parameterization of Wanninkhof (1992); we recalculated the CO_2 flux to be 1.73 ± 0.40 mol m^{-2} yr^{-1} by multiplying 0.44 (1 minus 0.56; see section 3.2). By conducting atmospheric eddy covariance measurements near the Bob Allen Keys (blue dot in Fig. 1), Van Dam et al. (2021) showed that the CO_2 flux in Florida Bay is 6.1–7.0 mol m^{-2} $year^{-1}$, which is higher than the corrected value of 1.73 ± 0.40 mol m^{-2} yr^{-1} in Zhang and Fischer (2014). Although the reason is not clear, primary production by phytoplankton and seagrasses might be lower when Van Dam et al. (2021) conducted their observation (2019–2020), resulting in higher CO_2 flux from sea to air, since there is no negative mean CO_2 flux in spring when they conducted their measurements (Fig. 1a in Van Dam et al., 2021). Van Dam et al. (2021) also calculated the excess CO_2, which is the CO_2 concentration difference between water and air to achieve the annual CO_2 flux of 6.1–7.0 mol m^{-2} $year^{-1}$, in Florida Bay to be between 5.2 and 6.0 µmol kg^{-1}, using a mean k of 11.7 cm h^{-1}; we recalculated the excess CO_2 to be between 14 and 16 μmol kg^{-1} using the k of 4.3 cm h^{-1}, which is parameterized from this study (Table 3). The recalculated excess CO_2 almost double their calculation of 5.2–6.0 μmol kg^{-1} and hence require more CO_2 input.

4. Summary

Air-sea gas exchange was investigated in a seagrass ecosystem using the ^3He and SF_6 dual tracer technique. The gas transfer velocity was lower than that in other coastal areas and open oceans, and commonly-used parameterizations tend to overpredict the gas transfer velocity, especially when wind was relatively strong. A new wind speed/gas exchange parameterization was proposed ($k(600) = 0.143u_{10}^2$), which fitted well to the observed gas exchange. This result suggests that wind is the dominant factor controlling gas exchange in the studied seagrass ecosystem. To assess the wider applicability of the proposed wind speed/gas exchange parameterization, more tracer release experiments are needed at similar inland ecosystems.

Data availability

The data used for this article is found at https://doi.org/10.5281/zenodo.6730934. Click “Version Florida 10.5281/zenodo.7087773” in the right column.

Author contributions

DH conceived, designed, and conducted the experiment. RD performed the data analysis.

Competing interests

The authors have declared that they have no competing interests.

Disclaimer

Acknowledgements

We thank Nicholas Chow, Nathalie Coffineau, Benjamin Hickman, and Lindsey Visser for assistance in the field, Peter Schlosser for measuring the ^3He samples, Rik Wanninkhof for guidance on the Schmidt number calculations, Damon Rondeau at Everglades National Park for providing data on wind, temperature, salinity, and tide, Pierre Polsenaere and an anonymous reviewer for helpful comments.

Financial support

Funding was provided by the National Aeronautics and Space Administration (NNX14AJ92G).

Review statement

References

Amorocho, J., and DeVries, J. J.: A new evaluation of the wind stress coefficient over water surfaces. *Journal of Geophysical Research: Oceans*, *85*(C1), 433-442, 1980

Atmane, M. A., Asher, W. E., and Jessup, A. T.: On the use of the active infrared technique to infer heat and gas transfer velocities at the air-water free surface. *Journal of Geophysical Research: Oceans*, *109*(C8), 2004

De Bruyn, W. J., and Saltzman, E. S.: Diffusivity of methyl bromide in water. Mar. Chem. 57:55-59. doi:10. 1016/S0304-4203(96)00092-8, 1997

DOE.: *Handbook of Methods for the Analysis of the Various Parameters of the Carbon Dioxide System in Sea Water, Version 2*, edited by A. G. Dickson and C. Goyet, ORNL/CDIAC-74, 1994

Duarte, C. M., Middleburg, J. J., and Caraco, N.: Major role of marine vegetation on the oceanic carbon cycle. *Biogeosciences* **2**: 1–8, 2005

Fourqurean, J. W., and others.: Seagrass ecosystems as a globally significant carbon stock. Nat. Geosci. 5: 505–509. doi:10.1038/ngeo1477, 2012

Ho, D. T., & Wanninkhof, R.: Air-sea gas exchange in the North Atlantic: 3He/SF6 experiment during GasEx-98. Tellus Series B, 68(1), 30198. https://doi.org/10.3402/tellusb.v68.30198, 2016

Ho, D. T., Asher, W. E., Bliven, L. F., Schlosser, P., & Gordan, E. L.: On mechanisms of rain-induced air-water gas exchange. Journal of Geophysical Research: Oceans, 105(C10), 24045-24057, 2000

Ho, D. T., Bliven, L. F., Wanninkhof, R. I. K., & Schlosser, P.: The effect of rain on air-water gas exchange. Tellus B, 49(2), 149-158, 1997a

Ho, D. T., Ho, Wanninkhof, R., Masters, J., Feely, R. A., and Cosca, C. E.: Measurements of underway fCO_2 in the eastern equatorial Pacific on NOAA ships Malcolm Baldridge and Discoverer from February to September, 1994, *Rep. ERL AOML-30*, 52 pp., NTIS, Springfield, Va, 1997b

Ho, D. T., Schlosser, P., & Caplow, T.: Determination of longitudinal dispersion coefficient and net advection in the tidal Hudson River with a large-scale, high resolution SF_6 tracer release experiment. *Environmental Science & Technology*, **36**(15), 3234–3241. doi:10.1021/es015814+, 2002

Ho, D. T., Law, C. S., Smith, M. J., Schlosser, P., Harvey, M., and Hill, P.: Measurements of air-sea gas exchange at high wind speeds in the Southern Ocean: Implications for global parameterizations, Geophys. Res. Lett., 33, L16611, doi:10.1029/2006GL026817, 2006

Ho, D. T., Coffineau, N., Hickman, B., Chow, N., Koffman, T. and Schlosser, P.: Influence of current velocity and wind speed on air-water gas exchange in a mangrove estuary, Geophys. Res. Lett., doi:10.1002/2016GL068727, 2016

Ho, D. T., De Carlo, E. H., and Schlosser, P.: Air-sea gas exchange and CO_2 fluxes in a tropical coral reef lagoon. J. Geophys. Res. Oceans 123: 8701–8713. doi:10.1029/2018JC014423, 2018a

Ho, D. T., Engel, V. C., Ferrón, S., Hickman, B., Choi, J., & Harvey, J. W.: On factors influencing air-water gas exchange in emergent wetlands. Journal of Geophysical Research: Biogeosciences, 123(1), 178–192. https://doi.org/10.1002/2017JG004299, 2018b

Howard, J.L., Creed, J.C., Aguiar, M.V.P., Fourqurean, J.W.: CO_2 released by carbonate sediment production in some coastal areas may offset the benefits of seagrass "Blue Carbon" storage. Limnol Oceanogr 63: 160–172. doi:https://doi.org/10.1002/lno.10621, 2017

Hayduk, W., & Laudie, H.: Prediction of diffusion coefficients for nonelectrolytes in dilute aqueous solutions. AIChE Journal, 20(3), 611–615. https://doi.org/10.1002/aic.690200329, 1974

Jähne, B., Munnich, K. O., Bosinger, R., Dutzi, A., Huber, W., & Libner, P.: On the parameters influencing air-water gas exchange. *Journal of Geophysical Research*, **92**, 1937–1949. https://doi.org/10.1029/JC092iC02p01937, 1987

King, D. B., & Saltzman, E. S.: Measurement of the diffusion coefficient of sulfur hexafluoride in water. *Journal of Geophysical Research*, **100**, 7083–7088. https://doi.org/10.1029/94jc03313, 1995

Lavrentyev, P. J., Bootsma, H. A., Johengen, T. H., Cavaletto, J. F., & Gardner, W. S.: Microbial plankton response to resource limitation: insights from the community structure and seston stoichiometry in Florida Bay, USA. Marine Ecology Progress Series 165: 45–57, 1998

Ledwell, J. R.: The variation of the gas transfer coefficient with molecular diffusivity. In W. Brutsaert, & G. H. Jirka (Eds.), *Gas transfer at water surfaces* (pp. 293–302). Hingham, MA: Reidel. https://doi.org/10.1007/978-94-017-1660-4_27, 1984

Ludin, A., Weppernig, R., Bönisch, G., & Schlosser, P.: Mass spectrometric Measurementmeasurement of helium isotopes and tritium in water samples, *Technical Report Rep. 98–6*, 42 pp, Lamont-Doherty Earth Observatory, Palisades, NY, 1998

Mcleod, E., Chmura, G. L., Bouillon, S., Salm, R., Björk, M., Duarte, C. M., ... & Silliman, B. R.: A blueprint for blue carbon: toward an improved understanding of the role of vegetated coastal habitats in sequestering CO2. *Frontiers in Ecology and the Environment*, *9*(10), 552-560, 2011

Nightingale, P. D., Malin, G., Law, C. S., Watson, A. J., Liss, P. S., Liddicoat, M. I., Boutin, J., and Upstill-Goddard, R. C.: In situ evaluation of air-sea gas exchange parameterizations using novel conservative and volatile tracers, Global Biogeochem. Cycles, 14, 373–387, doi:10.1029/1999GB900091, 2000

Philips, E. J., and Badylak, S.: Spatial variability in phytoplankton standing crop and composition in a shallow inner-shelf lagoon, Florida Bay, Florida, Bull. Mar. Sci., 58, 203–216, 1996

Phlips, E. J., Badylak, S. and Lynch, T. C.: Blooms of picoplanktonic cyanobacterium Synechococcus in Florida Bay, a subtropical inner-shelf lagoon. Limnol. Oceanogr., 44, 1166–1175, 1999

Pierrot, D., Neill, C., Sullivan, K., Castle, R., Wanninkhof, R., Lüger, H., ... & Cosca, C. E.: Recommendations for autonomous underway pCO2 measuring systems and data-reduction routines. *Deep Sea Research Part II: Topical Studies in Oceanography*, *56*(8-10), 512-522, 2009

Prager, E. J., and Halley, R. B.: The influence of seagrass on shell layers and Florida Bay mudbanks. *Journal of Coastal Research* 15: 1151–1162, 1999

Raymond, P. A., and Cole, J. J.: Gas exchange in rivers and estuaries: choosing a gas transfer velocity, Estuaries, 24, 269–274, doi:10.2307/1352954, 2001

Saltzman, E. S., King D. B., Holmen, K., and Leck, C.: Experimental determination of the diffusion coefficient of dimethylsulfide in water. J. Geophys. Res. 98:16481-16486 doi:10.1029/93JC01858, 1993

Schorn, S., Ahmerkamp, S., Bullock, E., Weber, M., Lott, C., Liebeke, M., ... and Milucka, J.: Diverse methylotrophic methanogenic archaea cause high methane emissions from seagrass meadows. *Proceedings of the National Academy of Sciences*, *119*(9), e2106628119, 2022

Sharqawy, M. H., Lienhard, J. H., & Zubair, S. M.: Thermophysical properties of seawater: a review of existing correlations and data. *Desalination and water treatment*, *16*(1-3), 354-380, 2010

Sogard, Powell, G. V. N., & Holmquist, J. G.: Spatial Distribution and Trends in Abundance Of Fishes Residing in Seagrass Meadows on Florida Bay Mudbanks. Bulletin of Marine Science, 44(1), 179–199, 1989

Stauffer, R. E.: Windpower time series above a temperate lake. Limnology and Oceanography, 25(3), 513-528, 1980

Takahashi, T., Olafsson, J., Goddard, J. G., Chipman, D. W., & Sutherland, S. C.: Seasonal variation of CO_2 and nutrients in the high-latitude surface oceans: A comparative study. *Global Biogeochemical Cycles*, *7*(4), 843-878, 1993

Van Dam, B. R., Lopes, C. C., Polsenaere, P., Price, R. M., Rutgersson, A., & Fourqurean, J. W.: Water temperature control on CO_2 flux and evaporation over a subtropical seagrass meadow revealed by atmospheric eddy covariance. Limnology & Oceanography, 66, 1–18. https://doi.org/10.1002/lno.11620, 2020

Van Dam, B. R., Zeller, M.A., Lopes, C., Smyth, A.R., Böttcher, M.E., Osburn, C.L., Zimmerman, T., Pröfrock, D., Fourqurean, J. W., Thomas, H.: Calcification-driven CO_2 emissions exceed “Blue Carbon” sequestration in a carbonate seagrass meadow, Res. Square, 10.21203/rs.3.rs-120551/v1, 2021

Wang, J. D., van deKreeke, J., Krishnan, N., Smith, D.: Wind and tide response in Florida Bay, *Bull. Mar. Sci.*, **54**, 579–601, 1994

Wang, J. D.: Subtidal flow patterns in western Florida Bay, *Estuarine Coastal Shelf Sci.*, **46**, 901–915, 1998.

Wanninkhof, R.: Relationship between gas exchange and wind speed over the ocean, J. Geophys. Res., 97, 7373–7381, doi:10.1029/92JC00188, 1992

Wanninkhof, R.: Relationship between wind speed and gas exchange over the ocean revisited. *Limnology and Oceanography: Methods*, **12**(6), 351–362. https://doi.org/10.4319/lom.2014.12.351, 2014

Wanninkhof, R., and Thoning, K.: Measurement of fugacity of CO2 in surface water using continuous and discrete sampling methods, Mar. Chem., 44, 189–205, 1993

Wanninkhof, R., Ledwell, J. R., Broecker, W. S., & Hamilton, M.: Gas exchange on Mono Lake and Crowley Lake, California. *Journal of Geophysical Research*, **92**, 14,567–14,580. https://doi.org/10.1029/JC092iC13p14567, 1987

Wanninkhof, R., Asher, W., Weppernig, R., Chen, H., Schlosser, P., Langdon, C., and Sambrotto, R.: Gas transfer experiment on Georges Bank using two volatile deliberate tracers, *J. Geophys. Res.*, **98**, 20,237–20,248, 1993

Wanninkhof, R., Asher, W. E., Ho, D. T., Sweeney, C., and McGillis, W. R.: Advances in quantifying air-sea gas exchange and environmental forcing, Annu. Rev. Mar. Sci., 1, 213–244, doi:10.1146/annurev.marine.010908.163742, 2009

Weiss, R. F.: Carbon dioxide in water and seawater: The solubility of a nonideal gas, *Mar. Chem.*, **2**, 203–215, 1974

Wilke, C. R., & Chang, P.: Correlation of diffusion coefficients in dilute solutions. *AIChE Journal*, *1*(2), 264–270. https://doi.org/10.1002/aic.690010222, 1955

Yates, K. K., Dufore, C., Smiley, N., Jackson, C., and Halley, R. B.: Diurnal variation of oxygen and carbonate system parameters in Tampa Bay and Florida Bay. *Mar. Chem*. 104, 110–124. doi: 10.1016/j.marchem.2006.12.008, 2007

Zhang, J.-Z., and Fischer, C. J.: Carbon dynamics of Florida Bay: Spatiotemporal patterns and biological control. Environ. Sci. Technol. 48: 9161−9169. doi:10.1021/es500510z, 2014

Zheng, M., De Bruyn, W. J., and Saltzman. E. S.: Measurements of the diffusion coefficients of CFC-11 and CFC12 in pure water and seawater. J. Geophys. Res. 103:1375- 1379. doi:10.1029/97JC02761, 1998

Zieman, J. C., Fourqurean, J. W., and Iverson, R. L.: Distribution, abundance and productivity of seagrasses and macroalgae in Florida Bay. Bull. Mar. Sci. 44: 292–311, 1989

Zieman, J. C., Fourqurean, J. W., and Frankovich, T. A.: Seagrass die-off in Florida Bay: long-term trends in abundance and growth of turtle grass, Thalassia testudinum. *Estuaries*, *22*(2), 460-470, 1999